chemosensors

Article

Progress in Fast and Red Plastic Scintillators

Matthieu Hamel

Université Paris-Saclay, CEA, List, F-91120 Palaiseau, France; matthieu.hamel@cea.fr

Abstract: Radiological detection where Cherenkov residual background can be prominent requires scintillators with increased emission wavelength. Cherenkov residual background precludes the use of UV-emitting sensors such as plastic scintillators. However, the literature is scarce in red-emitting plastic scintillators and only one commercial scintillator is currently available (BC-430, from Saint-Gobain Crystals and Detectors). In addition, X-ray imaging or time-of-flight positron emission tomography (ToF-PET) applications are also demanding on this type (color) of scintillators, but such applications also require that the material displays a fast response, which is not particularly the case for BC-430. We present herein our latest developments in the preparation and characterization of fast and red plastic scintillators for this application. Here, 'fast' means nanosecond range decay time and 'red' is an emission wavelength shifted towards more than 550 nm. At first, the strategy to the preparation of such material is explained by decomposing the scintillator to fundamental elements. Each stage is then optimized in terms of decay time response, then the elemental bricks are arranged to give plastic scintillator formulations that are compatible with the abovementioned characteristics. The results are compared with the red-emissive BC-430 commercial plastic, and the ultra-fast, violet-emitting BC-422Q 1% plastic. In particular, the first-time use of *trans*-4-dimethylamino-4′-nitrostilbene in the scintillation field as a red wavelength shifter allowed preparing plastic scintillators with the following properties: λ_{em}^{max} 554 nm, photoluminescence decay time 4.2 ns, and light output ≈ 6100 ph/MeV. This means a scintillator almost as bright as BC-430 but at least three times faster. This new sensor might provide useful properties for nuclear instrumentation.

Keywords: plastic scintillator; TCSPC; scintillation; DANS

Citation: Hamel, M. Progress in Fast and Red Plastic Scintillators. *Chemosensors* **2022**, *10*, 86. https://doi.org/10.3390/chemosensors10020086

Academic Editor: Nicole Jaffrezic-Renault

Received: 21 January 2022
Accepted: 16 February 2022
Published: 17 February 2022

1. Introduction

Various nuclear experiments are seeking to new detectors. The quest for new particles or improved detection efficiency is a trade-off with more constraints, thus pushing to rubbish standard, yet efficient detectors, to be replaced by new, application-driven detectors. This is the place where material chemists step in, at least in the world of nuclear instrumentation. Among the possible emission-wavelength variations of scintillators, red emitters are probably the ones with less demand [1]. Everybody knows and uses scintillators with standard emission wavelength, that is to say emitting close to 425 nm. Green-emitting plastic scintillators are useful when coupling to silicon photodiodes has to be achieved or when radiation-hard materials are necessary [2]. This being said, red-emitting scintillators are not commonly studied in this field, despite the fact they find relevant applications in physics domains, such as in the study of transient nuclear phenomena [3]. Other examples of the use of red and fast plastic scintillators may include: plastic scintillator dosimetry [4], ToF-PET [5] (when the scintillator also contains high-Z elements), real time X-ray imaging [6], and high-energy physics such as the Laser Mégajoule [7]. This last industrial application constitutes the birth of this work since red and fast plastic scintillators are the candidate of choice for the detection of low-energy X-rays.

The Cherenkov radiation spectrum is continuous and its intensity is inversely related to the square of the emission wavelength. So as to reduce or even avoid it in the counting of the incident dose rate (for example in dosimetry), it is thus necessary to work with wavelengths usually more than 550 nm. Table 1 summarizes some interesting scintillators and their main properties [8]. YAG:Ce is the only inorganic scintillator given for comparison. Its main drawback is the long decay time that precludes its use when fast counting or timing resolution are needed. BC-430 plastic scintillator is red-emitting and has a good light yield but its decay time might still be too long for some applications. To the best of our knowledge, the first red-emitting scintillator showing a fast decay time ever reported in the literature was prepared by Berlman and Ogdan [9]. This material was composed of a photonic cascade starting with 2-([1-biphenyl]-4-yl)-5-(*p*-*tert*-butylphenyl)-1,3,4-oxadiazole (butyl-PBD), 1,4-bis(5-(*o*-tolyl)oxazol-2-yl)benzene (dimethylPOPOP), perylene, and rubrene, all these fluorophores being hosted in polystyrene. Their trick was to irradiate the scintillator with electrons created from a LINAC, thereby reducing the 35 ns preliminary decay time down to 5 ns only by molecular degradation. However, the scintillator revealed to recover from irradiation (as they use to be [10]) and the decay time reincreased accordingly. Since this seminal paper, several strategies have been tested towards the preparation of new red-emitting plastics (Table 1), with the use of organic fluorophores showing high-range aromaticity or internal Förster energy transfer, organometallics, BODIPY or xanthene derivatives, or more recently with organic molecules showing thermally activated delayed fluorescence (TADF). Noteworthy, our laboratory published some years ago their preliminary results on such chemical modifications for new red and fast plastics [11]. Thus, a polystyrene-based scintillator including 2,5-diphenyloxazole, Nile Red, and piperidine as the quencher displayed low scintillation yield and moderate decay time but at high wavelength (more than 600 nm).

This publication presents our latest results on this field. It is decomposed as follows. The choice of the primary and the secondary fluorophores was performed independently, then ternary mixtures (matrix + primary fluorophore + secondary fluorophore) were studied, eventually with the addition of a photoluminescent quencher. All these sequences are presented and discussed individually. In particular, the introduction of a new red-emitting fluorophore in the scintillation field provides new insights and acceptable characteristics for a red and fast plastic scintillator. Thus, a plastic scintillator consisting in polystyrene, *p*-terphenyl and *trans*-4-dimethylamino-4′-nitrostilbene displayed adequate photophysical characteristics and a decent light output, close to BC-430.

Table 1. Main plastic and liquid scintillators. Only scintillators operating at $\lambda_{em}^{max} > 550$ nm are cited. The list is sorted in ascending emission wavelength.

State	Last Fluorophore	λ_{em}^{max} (nm)	Light Output (ph/MeV)	Decay Time (ns)[c]	Ref.
YAG:Ce	$Y_3Al_5O_{12}$(Ce)	550	8000	70	-
PVT scintillator	BC-430	580	6900	16.8	-
Polymer thin film	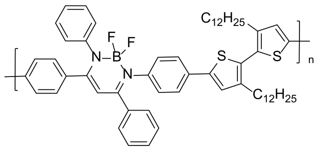	584	n.d. [a]	0.46 (60) + 1.0 (40)	[12]
Polystyrene scintillator	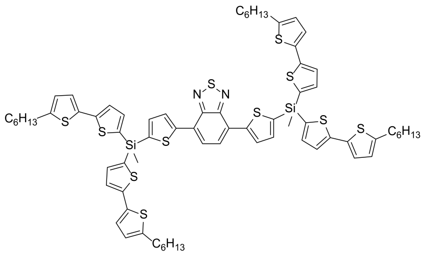	588	9780	n.d.	[13]
Polystyrene scintillator	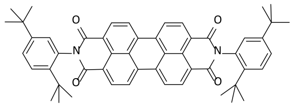	591	80	9.22–13.26	[7]
Polystyrene scintillator	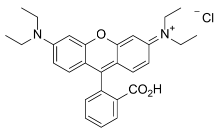	595	n.d.	5.94	[14]
Polystyrene scintillator	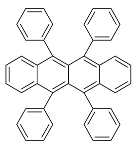	>600	n.d.	5	[9]
Polysiloxane scintillator	Lumogen Red	≈600	8300	n.d.	[15]
Polystyrene scintillator	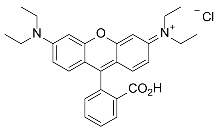	600	≈16,000	≈6	[3]

Table 1. *Cont.*

State	Last Fluorophore	λ_{em}^{max} (nm)	Light Output (ph/MeV)	Decay Time (ns)[c]	Ref.
PMMA scintillator	$CsPbBr_3$ Perovskite + 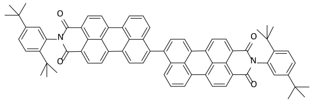	≈600	≈9000	3.4 (87) + 14.1 (13)	[5]
Poly(styrene-*co*-acrylonitrile) scintillator	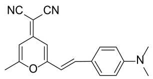	≈610	n.d.	n.d.	[16]
Polystyrene scintillator	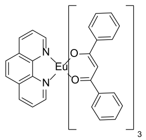	614	5650 [b]	469,000	[17]
Sucrose octaacetate	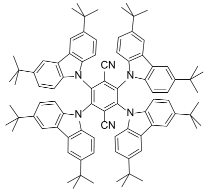	618	37,500	10.9 + 1960	[6]
Polystyrene scintillator	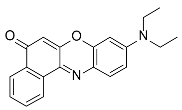	610–620	70–300	8.7	[11]
PMMA scintillator	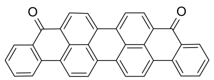	≈620	n.d.	3.94	[18]
Polymer in liquid	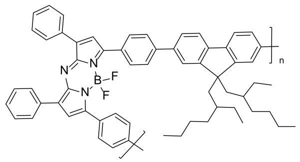	750	n.d.	1.92	[19]

[a] n.d.—not determined. [b] value obtained from ^{239}Pu alpha excitation. [c] usually monoexponential. When it is biexponential, it is expressed at the percentage of the first and the second exponential in the global fit.

2. Materials and Methods

2.1. Materials

All chemicals were purchased from Sigma-Aldrich, except for PMP and *p*-sexiphenyl that were obtained from TCI Europe Research Chemicals. Styrene and vinyltoluene were distilled prior to use. 4-Bromo-*p*-terphenyl was prepared according to a published procedure [20]; a white powder was obtained with an 80% yield after purification. *N*-(2-ethylhexyl carbazole) was prepared according to our previous work [21]. Spectroscopic toluene was obtained from Carlo Erba. BC-430 and BC-422Q 1% and 2% plastic scintillators were obtained from Saint-Gobain Crystals and Detectors; unfortunately, their purchase date is not known and one has to keep in mind that BC-422Q may suffer from aging with time [22]. All monomers and amines were vacuum-distilled before use, monomers being also dried over calcium hydride. Liquid scintillators were prepared by dissolving the dyes into spectroscopic toluene and were neither degassed nor saturated with neutral gas. The reason is twofold: the presence of oxygen decreases the decay time, and the saturation with neutral gas is modified by oxygen diffusion within the liquid. Plastic scintillators were prepared according to our internal procedure, except the fact that the monomers were not degassed prior to polymerization. After heating the monomer with the suitable molecules until complete polymerization, the raw material was cut and polished until obtaining a plastic scintillator with dimensions 49 mm diameter and 30 mm thickness (unless otherwise stated), which are equivalent to the size of BC-422Q 1% (Φ 50 mm, h 10 mm) or BC-430 (Φ 50 mm, h 50 mm) used as reference materials.

2.2. Methods

Fluorescence spectra were recorded with a Fluoromax 4P spectrofluorometer (Horiba Jobin Yvon, Palaiseau, France) monitored with FluorEssence software. Fluorescence spectra were recorded orthogonally to the excitation light. A time correlated single photon counting (TCSPC) module was used to record the lifetime of the samples. Two different excitation wavelengths were used, 274 nm and 368 nm, with pulse widths <1.2 ns. In liquid state, TCSPC analyses were performed in standard $1 \times 1 \times 3$ cm^3 quartz cuvettes with the emission recorded at 90° from the excitation diode. Plastic scintillators were excited on their cylindrical edge, approximately at a depth of 0.5 cm away from the flat face, the latter being directed toward the photodetector of the spectrofluorometer. Decay spectra were fitted using the DAS6 software (Horiba Jobin Yvon). In each case, a biexponential fit was adjusted so that the χ^2 was in the range 1.00–1.20. The instrument response function was recorded by replacing the sample with a 3 cm^3 quartz cuvette filled with Ludox®. The mean decay times are given with two decimals, for a better comparison between the materials. Radioluminescence spectra were acquired according to our latest published experimental procedure [2] with a beta-emitting ^{90}Sr/^{90}Y source (31.9 MBq as of November 2020).

The absorption characteristics of molecules were recorded with an Cary 60 UV–vis spectrophotometer (Agilent, Les Ulis, France), with an optical path of 1 cm.

Pulse-height spectra were obtained as follows. In a black box, the scintillator was coupled with optical grease to a blue-sensitive R6231 photomultiplier tube (Hamamatsu, Massy, France) or a red-sensitive 9202SB photomultiplier tube (ET Enterprises, Uxbridge, UK), depending on the scintillator to be tested, operating at +1100 V or −1700 V, respectively. The anode fed a DT5730SB digitizer from CAEN. A ^{137}Cs source (gamma ray, 500 kBq as of November 2020) located ca. 10 cm away from the scintillator or a ^{36}Cl source (beta emitter, 6 kBq as of November 2020) placed on the top of the scintillator were used, and the obtained pulse height spectrum was recorded during 500 s.

3. Results and Discussion

Fast and red plastic scintillators can be decomposed into the following components: polymer, fluorophores, and—if necessary—photoluminescence quencher. Each elemental brick was individually examined to allow a better understanding on possible limitations or improvements. Polystyrene or poly(vinyltoluene) were considered as the polymer building block since they are very well-known polymers and are the ones used in the composition of almost all commercial plastic scintillators [1]. No other polymers were considered in this study. In addition, thermally-assisted radical polymerization was used to polymerize the suitable, highly purified monomers.

To get more rationale on the results and insight into each chemical's role, binary mixtures, that is to say matrix + primary fluorophore or matrix + secondary fluorophore were studied first. Each fluorophore indeed has its solvent-dependent photophysical properties (emission wavelength and more particularly herein decay time) and has to be experimentally assessed. The 'Holy Grail' would be a fluorophore combination presenting the desired time characteristics, in other words without necessity to quench their photoluminescence with extra molecules. This would afford a highly scintillating, time-stable, yet fast plastic scintillator.

It is noteworthy that the shape, thickness, and coating of a scintillator have a large influence on its resulting decay time [23]. A 50% increase of the decay time can be observed when increasing the material's thickness from 0.2 to 5 cm [24]. The scintillator needs to be wrapped with black material to mitigate internal reflections. Intuitively, thinner scintillators afford the best timing properties. The purpose of our work was to find out the best chemical composition; no morphology improvement was therefore performed. This is why each table referencing timing properties of plastics mentions the diameter and the thickness of the studied materials.

3.1. Intrinsic Limitations of the Spectrofluorometer Setup

Our equipment uses two different Horiba Jobin Yvon NanoLED excitation sources that operates at either 274 nm or 368 nm (N-270 and N-370 LED heads, respectively) for time-correlated single photon counting experiments. This constitutes the main limitation of this study since these two diodes display typical pulse widths less than 1.2 ns, so close to the best decay times we are currently measuring and expecting (and even longer than commercial references BC-422Q 1% and 2%) [25]. One can see that the excitation profile is not purely monoexponential, with a bump appearing a few nanoseconds after the pulse. Their full-width at half maximum (FWHM) values are 1.48 ns $\pm$ 0.11 ns and 1.68 ns $\pm$ 0.11 ns. Without any access to better-resolved pulse diodes, the results are presented as such.

3.2. Matrix + Primary Fluorophore Mixtures

Such combinations have been widely documented and reviewed [24] by many pioneering works on plastic scintillator formulations. These so-called binary mixtures have proven to be the fastest decaying scintillators: adding a wavelength-shifter to the solution implies supplementary energy transfers that can occur both radiatively and non-radiatively. So as to perform a fast screening, various molecules suitable for scintillation purposes were solubilized in toluene at 1 wt %, and their photoluminescence decay time was recorded by time-correlated single photon counting (TCSPC) measurements.

Among other strategies [26], the intramolecular heavy atom quenching was assessed by adding one or two bromine atoms on the *para* positions of *p*-terphenyl. It seems that the fastest UV-emitting plastic scintillator ever described was prepared according to this approach [27]. Thus, 4-bromo-*p*-terphenyl was synthesized according to a published procedure [20]. According to Scheme 1, bromine reacted on *p*-terphenyl in a mixture of dichloromethane and trifluoroacetic acid and readily afforded 4-bromo-*p*-terphenyl with an 80% yield. Except *N*-(2-ethylhexylcarbazole) which was also prepared, all other tested molecules were used with commercial grade and no further purification. For all scintillators described thereafter, it is noteworthy that the solutions were not degassed so as to allow dissolved oxygen to act as a potential quencher of long-lived stated. The results of 19 different benchmarked molecules are given in Table 2. A non-linear fitting was chosen between single or biexponential decay so that the χ^2 fitting value was restricted to the range 1.00–1.20. Some of these molecules are known to display either a concentration-dependent (2,5-diphenyloxazole, *N*-(2-ethylhexyl)carbazole, pyrene), or an oxygen-sensitive (naphthalene, pyrene) decay time. Therefore, these results have to be considered as a fast qualitative survey of family of molecules that could be suitable to the foreseen application. The results show that phenylene- and PBD-derivatives are of particular interest in this context. In the oligophenylene series, the photoluminescence decay time shortens when increasing the number of phenyl groups, however at the expense of the solubility of the molecule.

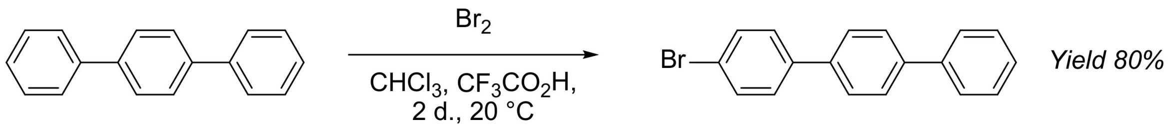

Scheme 1. Preparation of 4-bromo-*p*-terphenyl.

A possible photoluminescence quenching of *p*-terphenyl and *p*-quaterphenyl with benzophenone or hindered amines was also tested with piperidine or *N*,*N*-diisopropylethylamine (also known as Hünig's base). At least in the toluene medium (Table 3), all three quenchers proved their efficiency with the best results observed for *p*-terphenyl quenched with piperidine. Thus, starting with already fast materials (<τ> = 1.45 and 1.11 ns for *p*-terphenyl and *p*-quaterphenyl, respectively), quenching leads to decay values close to 1 ns, placing them in the range of the instrument response function provided by the NanoLED characteristics (Figure 1). At this stage, no care was taken on the photoluminescence or even scintillation efficiency.

We then turned our attention on binary plastic compositions of *p*-terphenyl, *p*-quaterphenyl, and 4-bromo-*p*-terphenyl, these fluorophores being eventually quenched with benzophenone. Table 4 resumes the photoluminescence properties of various plastic scintillators compared with BC-422Q 1% and 2% commercial plastic scintillators. According to the literature, these scintillators are assumed to be quenched with benzophenone. All scintillators are still UV-emitters, with BC-422Q 2% and PS *p*-T 2 B 2 (see Table 4 for the interpretation of this abbreviation) which are the two scintillators emitting at wavelengths more than 400 nm. This effect might be related to the use of 2% of benzophenone that absorbs part of the emitted light below 400 nm.

Among the scintillators listed in Table 4, the fastest formulations were compared in terms of radioluminescence spectra. Thus, each scintillator was exposed to a beta emitting ^{90}Sr/^{90}Y radioactive source, and their photoluminescence integral was compared with the same commercial plastics BC-422Q 1% and 2%. Table 5 gives the radioluminescence emission maximum (whose spectra are also given Figure 2), the normalized emission integral against BC-422Q 1% and the corresponding relative light yield, and another parameter we have recently introduced. This is the light intensity given by the combination of the pulse shape with the pulse amplitude, expressed in ph/MeV/ns [2]. The relative light yield was taken by pulse height spectrum using a ^{137}Cs gamma ray source using a standard pulse height spectrum setup.

For all compounds, a strong dependence of the decay time with the primary fluorophore's concentration is observed. Whereas PPO-based plastics have faster decays for low concentrations [11], herein *p*-quaterphenyl plastics are accelerated when increasing the concentration. The case of 4-bromo-*p*-terphenyl is more subtle. The decay lies between 2.95 ns and 3.31 ns between 0.5 and 1.5 wt %. At 3.5 wt %, the decay time and the light yield as well show a dramatic improvement, until reaching the performances of BC-422Q 1%, but with no quencher inside. It is noteworthy that at so high concentration 4-Br-*p*-T did not dissolve entirely as small aggregates were still visible. Even if not homogenous, this plastic scintillator could therefore become a suitable alternative to BC-422Q 1% for use with a long-term stability requirement because it does not embed any volatile quencher.

Table 2. Mono or biexponential fitting of the photoluminescence decay of molecules dissolved at 1 wt % in toluene (λ_{ex} = 274 nm; $\lambda_{obs} = \lambda_{em}^{max}$).

Molecule	Structure	Mono- or Biexponential τ (ns) [a]	<τ> (ns) [b]
PPO	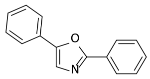	2.27	2.27
1,1,4,4-tetraphenylbutadiene	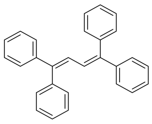	1.45 (99) + 34.7 (1)	1.78
Biphenyl	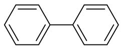	4.81	4.81
p-terphenyl	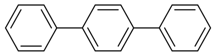	1.45	1.45
p-quaterphenyl	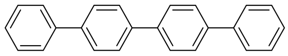	0.85 (73) + 1.82 (27)	1.11
p-sexiphenyl	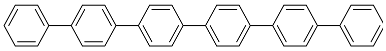	1.67 (66) + 2.83 (34)	2.06
m-terphenyl	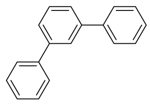	1.15 (59) + 8.96 (41)	4.35
4-bromo-*p*-terphenyl	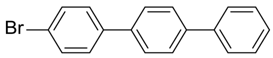	0.72 (58) + 3.81 (42)	2.01
4,4′-dibromo-*p*-terphenyl	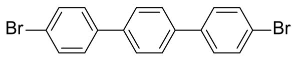	1.90 (64) + 12.54 (36)	5.73
*PMP*1-phenyl-3-(mesityl)-2-pyrazoline	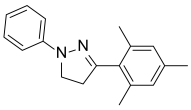	4.11	4.11
Naphthalene	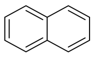	8.67	8.67
Anthracene	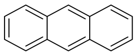	2.42 (90) + 8.51 (10)	3.03
4-isopropylbiphenyl	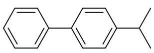	0.80 (5) + 4.94 (95)	4.73
Pyrene	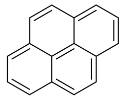	23.0	23.0
N-ethylcarbazole	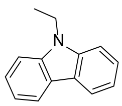	7.91	7.91
N-(2-ethylhexyl)carbazole	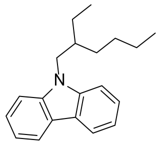	12.30	12.30
*BBD*2,5-di(4′-biphenylyl)-1,3,4-oxadiazole	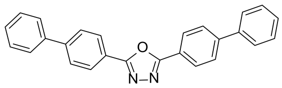	1.35	1.35
*PBD*2-phenyl-5-(4′-biphenylyl)-1,3,4-oxadiazole	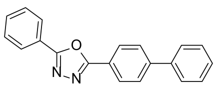	1.51	1.51
*Butyl-PBD*2-(*p*-*tert*-butylphenyl-5-(4′-biphenylyl)-1,3,4-oxadiazole	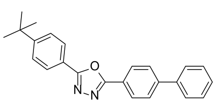	0.92 (54) + 1.64 (46)	1.25

[a] When the fitting of the decay curve proved to be better expressed as a biexponential, the results are given according to the following: τ_{fast} ($\%_{fast}$) + τ_{slow} ($\%_{slow}$). [b] $<\tau> = \tau_{fast} \times \%_{fast} + \tau_{slow} \times \%_{slow}$.

Table 3. Photoluminescence quenching of *p*-terphenyl or *p*-quaterphenyl with piperidine or benzophenone in toluene. λ_{ex} = 274 nm; λ_{obs} = 342 nm (*p*-Terphenyl) or 386 nm (*p*-Quaterphenyl).

Molecule	Quencher (wt %)	τ (ns)	<τ> (ns)
p-terphenyl	-	1.45	1.45
p-terphenyl	Benzophenone (0.4)	0.59 (63.5) + 1.85 (36.5)	1.05
p-terphenyl	Piperidine (1.6)	0.60 (71) + 1.92 (29)	0.98
p-terphenyl	Hünig's base (1.6)	0.66 (78.6) + 2.11 (21.4)	0.97
p-quaterphenyl	-	0.85 (73) + 1.82 (27)	1.11
p-quaterphenyl	Benzophenone (0.4)	0.77 (42.5) + 2.08 (57.5)	1.52
p-quaterphenyl	Piperidine (1.6)	1.73	1.73
p-quaterphenyl	Hünig's base (1.6)	0.71 (48.5) + 4.44 (51.5)	2.6

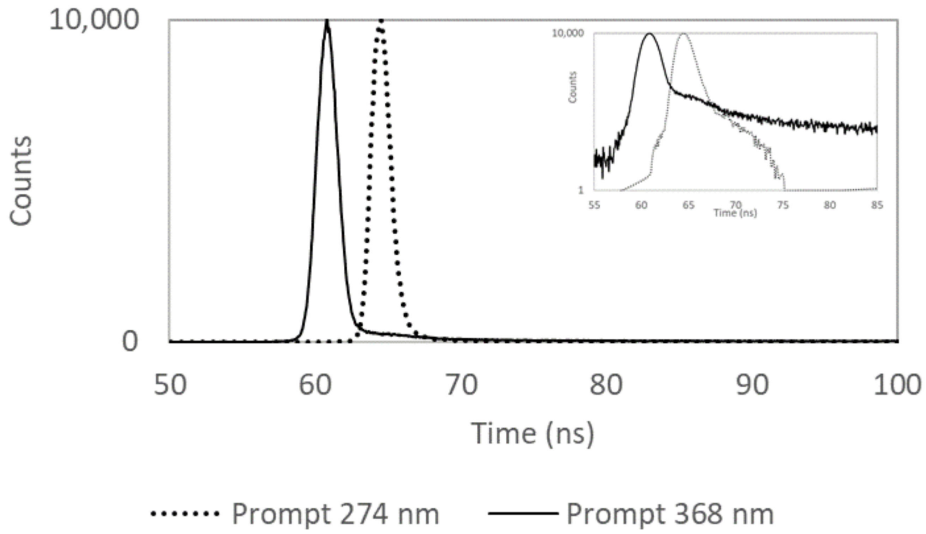

Figure 1. Excitation profiles of the two NanoLEDs used in this experiment, dashed line: 274 nm, solid line: 368 nm. Inset: focus on the afterpulses.

Table 4. Photoluminescence properties of several plastic-state binary mixtures, eventually quenched with benzophenone. λ_{ex} = 274 nm; $\lambda_{obs} = \lambda_{em}^{max}$. All scintillators are with dimension Φ 49 mm h 10 mm.

Composition *	Mono- or Biexponential τ (ns) *	<τ> (ns)	λ_{em}^{max} (nm)	FWHM (ns)
BC-422Q 1%	0.78 (67) + 3.05 (32)	1.52	360	2.05
BC-422Q 2%	0.81 (73) + 3.08 (27)	1.42	402	1.96
PVT *p*-Q 0.3	1.71 (52) + 11.6 (48)	6.46	370	2.58
PVT *p*-Q 0.6	1.50 (59) + 9.93 (41)	4.69	370	2.52
PVT *p*-Q 1.0	1.52 (66) + 8.41 (34)	3.86	370	2.52
PVT *p*-Q 0.6 B 0.6	1.23 (63) + 8.05 (37)	3.86	370	2.25
PS *p*-T 2 B 2	0.81 (48.5) + 4.09 (51.4)	2.50	410	2.08
PS 4-Br-*p*-T 0.5	0.56 (50) + 2.90 (34.9) + 10.9 (15.1)	2.95	400	1.71
PS 4-Br-*p*-T 1.0	0.99 (49.75) + 5.38 (50.25)	3.19	400	2.14
PS 4-Br-*p*-T 1.5	0.53 (46.5) + 2.80 (36.1) + 11.8 (17.4)	3.31	400	1.71
PS 4-Br-*p*-T 3.5	0.882 (73.9) + 4.00 (26.1)	1.69	400	2.00

* PVT: poly(vinyltoluene), PS: polystyrene, *p*-T: *p*-terphenyl, *p*-Q: *p*-quaterphenyl, 4-Br-*p*-T: 4-bromo-*p*-terphenyl, B: benzophenone. The numeral values of the first row are for the weight concentrations.

Table 5. Radioluminescence performances of selected plastic scintillators. All scintillators measure Φ 49 mm h 10 mm.

Composition *	$\lambda^{max}_{radiolum.} \pm 2$ **(nm)**	**Radioluminescence vs. BC-422Q 1% (%)**	**Light Yield ϕ vs. BC-422Q 1% (ph/MeV)**	**ϕ/<τ> (ph/MeV/ns)**
BC-422Q 1%	400	100	1700	1118
BC-422Q 2%	406	56	290	204
PVT *p*-Q 0.3	394	140	1940	300
PVT *p*-Q 0.6	402	118	1310	279
PVT *p*-Q 1.0	398	229	2840	735
PVT *p*-Q 0.6 B 0.6	396	87	610	158
PS 4-Br-*p*-T 1.0	394	52	700	219
PS 4-Br-*p*-T 3.5	396	90	1870	1106

* See Table 4 for abbreviations.

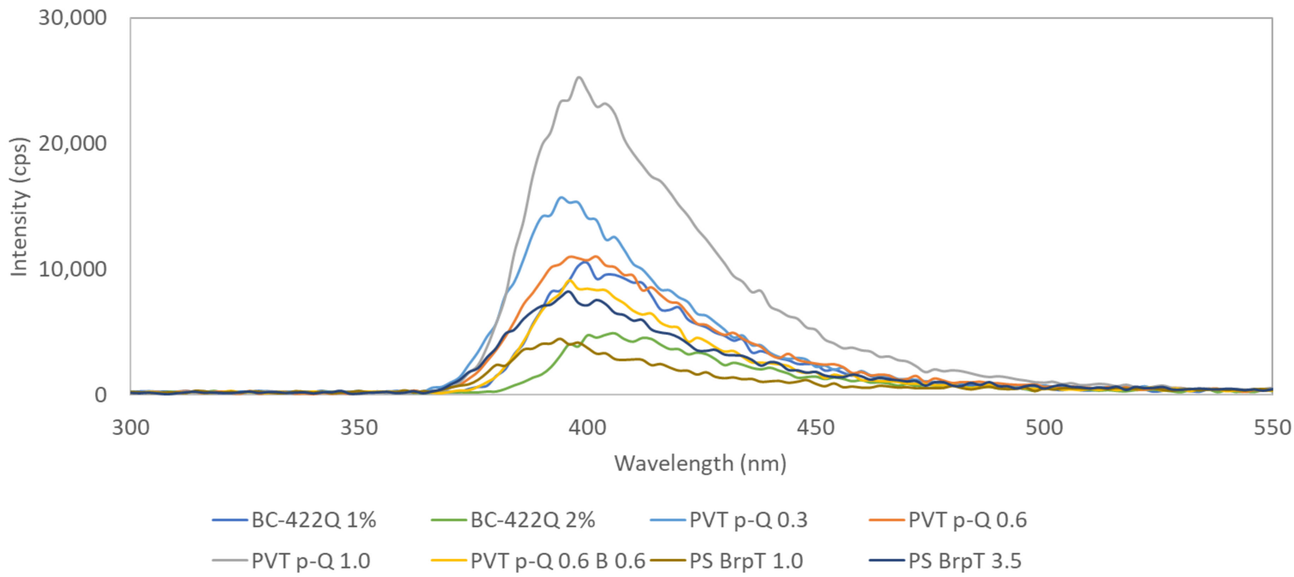

Figure 2. $^{90}Sr/^{90}Y$ radioluminescence of binary mixtures compared with commercial plastics.

3.3. Matrix + Secondary Fluorophore Mixtures

Intrinsically red-emitting fluorophores present slower decay times than UV-emitting fluorophores as a linear dependence of lifetime with the emission wavelength is predicted [8]. The same procedure as for primary fluorophores has been repeated, that is to say dissolving at low concentrations known red emitting fluorophores that are soluble in toluene, and to check their photoluminescence decay time thanks to TCSPC. The results are given in Table 6. Preliminary studies have shown that polar fluorophores could be added at a rather high concentration to give fast decaying liquid scintillators [28]. We decided to withdraw this strategy since the as-prepared scintillators with such high concentrations must present very strong self-absorption. Nile red was our primary candidate [11], despite its long decay time (27.3 ns). Rubrene was first used by Berlman et al. [9], the two perylenedicarboximide and the two pyrromethene derivatives that have been tested revealed to be too long-decaying, and the best observations were obtained with 4-(dicyanomethylene)-2-methyl-6-(4-dimethylaminostyryl)-4*H*-pyran (DCM) and 4-dimethylamino-4′-nitrostilbene (DANS). Molecules from the xanthene family (Eosin Y, Erythrosin B, Rhodamine derivatives) were also tested but displayed poor solubility in polar media such as toluene, polystyrene, or poly(vinyltoluene), even at the very low content we are looking at—typically 0.03 wt %. A second strategy was thus developed but not presented herein. Copolymers made from styrene and highly polar monomers were prepared along with the xanthene derivative. However, after several weeks, the materials usually degraded, deformed, and became cloudy. This degradation was, however, not mentioned in preceding literature [3,14].

Table 6. Main photophysical characteristics of red-emitting molecules dissolved at 0.03 wt % in air-saturated toluene solutions (λ_{ex} = 368 nm; $\lambda_{obs} = \lambda_{em}^{max}$).

#	Molecule	Structure	λ_{em}^{max} (nm)	τ (ns)
1	Nile red	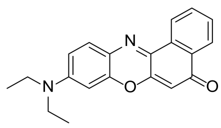	610	5.18
2	*DCM*4-(Dicyanomethylene)-2-methyl-6-(4-dimethylaminostyryl)-4*H*-pyran	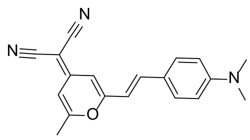	550	0.95
3	Rubrene	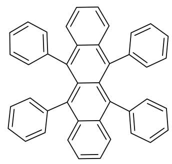	584	27.3
4	*N*,*N*′-Bis(2,5-di-*tert*-butylphenyl)-3,4,9,10-perylenedicarboximide	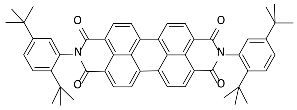	580	6.6
5	*N*,*N*′-Bis-*n*-pentyl-1,6,7,12-tetrachloro-3,4,9,10-perylenedicarboximide	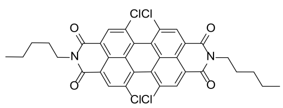	596	11.4
6	*Pyrromethene 605*Difluoro [2-(4-ethyl-3,5-dimethyl-1*H*-pyrrol-2-yl-κ*N*)-2-(4-ethyl-3,5-dimethyl-2*H*-pyrrol-2-ylidene-κ*N*)ethyl acetato])boron	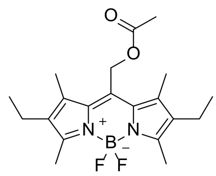	586	12.4
7	*Pyrromethene 597*Difluoro(4-(1,1-dimethylethyl)-2-{1-[4-(1,1-dimethylethyl)-3,5-dimethyl-2*H*-pyrrol-2-ylidene-*N*]ethyl}-3,5-dimethyl-1*H*-pyrrol-2-ylidene-*N*]ethyl}-3,5-dimethyl-1*H*-pyrrolato-*N*)boron	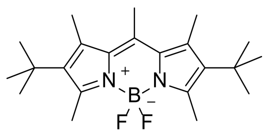	608	13.8
8	*DANSTrans*-4-dimethylamino-4′-nitrostilbene	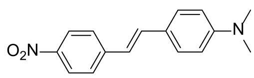	560	3.28

DCM is a molecule that exhibits considerable variability of its photoluminescence response regarding the polarity of the solvent it is dissolved in. DCM was already mentioned as a potential shifter for polystyrene-based scintillators [29]. Photoluminescent literature precedents [30] as well as laboratory measurements are resumed in Table 7. It turns out that, in apolar solvent, DCM is extremely fast-decaying, with an interesting emission wavelength for our given application ($\lambda_{em}^{max} \approx 550$ nm), albeit at the expense of the quantum yield, with toluene being the best example of such behavior. Accordingly, DCM in styrene was also tested. The observed 0.95 ns decay time must be limited by the timing resolution due to the pulse width excitation of our spectrofluorometer, so the decay time of DCM in styrene must be taken with caution. Experimental measurements in PMMA are in good agreement with literature precedents (lines 2 and 1, respectively). Unfortunately, plastic rigidity increases the photoluminescence decay time of DCM—whatever its concentration—towards a 3.8 ns value.

Table 7. Comparison of relevant photophysical data of DCM under various conditions.

Matrix		λ_{em}^{max} (nm)	τ (ns)	Quantum Yield
PMMA	Bibliography	550	2.0	0.76
PMMA	Measurement	550	2.63	n.d.
Toluene	Bibliography	567	0.02	0.08
Styrene	Measurement	550	0.95	n.d.
Polystyrene	Measurement	550	3.80	n.d.

n.d.: not determined.

The second molecule that is potentially interesting is *trans*-4-dimethylamino-4′-nitrostilbene (usually abbreviated as DANS), known as a push-pull chromophore [31]. To the best of our knowledge DANS has never been used in the scintillation field. The absorption maximum of a 0.002 wt % of DANS in toluene (i.e., 7.45×10^{-5} mol·L^{-1}) is located at 437 nm, with a calculated absorption molar coefficient of 22,600 L·mol^{-1}·cm^{-1} (literature 447 nm and 26,630 L·mol^{-1}·cm^{-1} in chlorobenzene [32]). This last value is adequate for a secondary fluorophore role as it falls between 9,10-diphenylanthracene (ε 14,000 L·mol^{-1}·cm^{-1}, cyclohexane [33]) and POPOP (ε 47,000 L·mol^{-1}·cm^{-1}, cyclohexane [33]) which are two wavelength shifters particularly used in scintillation. DANS displays a maximum of emission equal to 560 nm and a photoluminescence decay time of 3.28 ns at 0.002 wt % in toluene. This decay time value looks long compared with the 0.94 ns value for its lifetime reported in the literature [32]. This fast decay induces a low photoluminescence quantum yield (0.10 in chlorobenzene [32]), which may be reduced by a twisted intramolecular charge transfer. We also noticed that in toluene, this molecule is also sensitive to traditional quenchers, as can be seen in Table 8. Figure 3 gives the photoluminescence decay profiles of seven liquid scintillators being quenched with either benzophenone, piperidine, or the Hünig's base at concentrations of 1.6 wt % or 4.8 wt %. It was unexpected to see an afterglow appear for 'quenched' scintillators with benzophenone. In that case, not only is the prompt photoluminescence affected, but a delayed photoluminescence appears. This behavior is still unclear to our eyes. On the other hand, both piperidine and Hünig's base were efficient quenchers, with a quenching efficiency dependent with the quencher concentration, at least for the two studied concentrations. Figure 4 shows a time-resoled emission spectroscopy spectrum of DANS in toluene and quenched by Hünig's base. As such, the emission characteristics are perfect for our aimed application. Thus, DCM and DANS were selected as potent wavelength-shifters for the design of red and fast plastic scintillators.

Table 8. Quenching of *trans*-4-dimethylamino-4′-nitrostilbene with various quenchers. Solvent toluene. λ_{ex} = 368 nm; λ_{obs} = 560 nm.

Quencher	Concentration (wt %)	τ (ns)	<τ> (ns)	FWHM ± 0.05 (ns)
-	0	3.28		5.00
Benzophenone	1.6	3.37		4.78
Benzophenone	4.8	3.44 (89.1) + 61.1 (10.9)	9.72	4.72
Piperidine	1.6	2.02		3.13
Piperidine	4.8	0.91 (72.8) + 2.39 (27.2)	1.31	2.25
Hünig's base	1.6	2.16		3.24
Hünig's base	4.8	1.17 (91.8) + 5.14 (8.2)	1.50	2.41

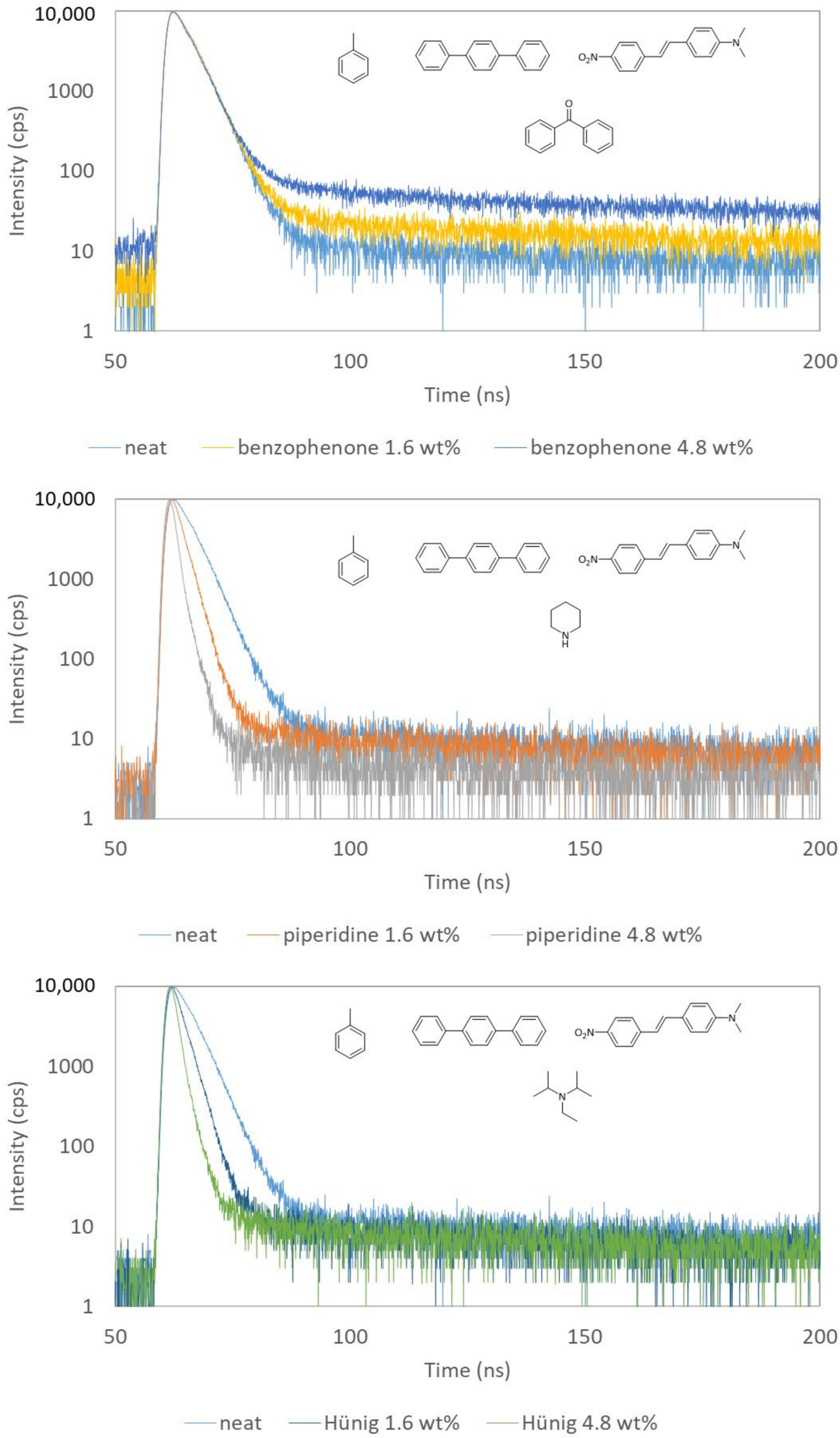

Figure 3. Photoluminescence quenching of a plastic scintillator composed of PS + *p*-terphenyl 1.5 wt % + DANS 0.01 wt % with different amounts of benzophenone (**top**), piperidine (**middle**), or Hünig's base (**bottom**). The same unquenched, reference material is added on each figure in light blue color (τ_{ex} = 274 nm; τ_{obs} = 560 nm).

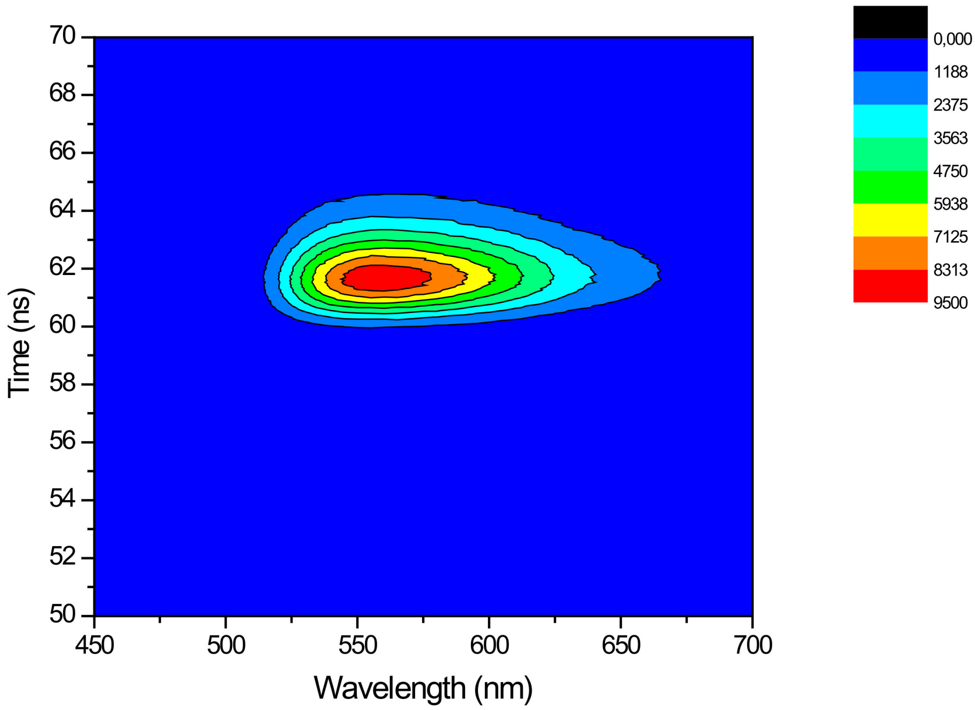

Figure 4. Time-resolved emission spectroscopy of 0.03 wt % 4-dimethylamino-4′-nitrostilbene in toluene, quenched with 5 wt % of Hünig's base. τ_{mean} = 1.50 ns (λ_{ex} = 368 nm).

3.4. Full Red-and-Fast Plastic Systems

To resume, *p*-terphenyl or its 4-brominated derivative have been chosen as primary fluorophores, when DCM and *trans*-4-dimethylamino-4′-nitrostilbene can be useful as secondary fluorophores. Plastic scintillators were thus prepared, starting from polystyrene as the matrix. In addition, several other secondary fluorophores that were presented in Table 6 were also benchmarked. All secondary fluorophores were tested at three different weight concentrations, from 0.01 wt % up to 0.05 wt %. The results are summarized in Table 9.

The first observation is the fact the DANS-based scintillators are not as fast as their liquid equivalents, with TCSPC values giving around 4 ns. This was already observed for Nile red-based scintillators [11]. The radioluminescence spectra show emission wavelengths that are in agreement with the photoluminescence spectra.

The determination of the light output of the scintillators was performed either with a radioluminescence setup ($^{90}Sr/^{90}Y$ excitation) or with a more traditional pulse-height spectrum methodology (^{36}Cl excitation). In both cases, beta emitters were used, and the plastic scintillators were benchmarked against BC-430 commercial plastic. This light output is then divided by the mean decay value, which gives the number of photons per deposited energy per time. This parameter is thus the best parameter for most applications, and it favors very fast materials. Here, BC-430 and BC-422Q 1% afford 552 and 1118 ph/MeV/ns, respectively. The best results for our prepared scintillators were obtained with the DANS-based scintillators, with a value of the same order of magnitude as for BC-422Q 1%. The weakest materials were the DCM-based since the quantum yield of DCM in polystyrene is too low.

Table 9. Photoluminescence and scintillation properties of red and fast plastic scintillators compared with BC-430 and BC-422Q 1%. For the TCSPC values: λ_{obs} = 560 nm. All scintillators are with dimension Φ 49 mm h 30 mm, except BC-430 which is Φ 50 mm h 50 mm, and BC-422Q 1% which is Φ 50 mm h 15 mm.

Plastic Scintillator [a]	λ_{em}^{max}**(nm)** [b]	**τ (ns)** λ_{ex} **274 nm**	**FWHM ± 0.11 (ns)**	**ϕ (ph/MeV)** [c]	**ϕ (ph/MeV)** [d]	**ϕ/<τ> (ph/MeV/ns)** [e]
BC-430	580	12.5	23.00	6900	6900	552
BC-422Q 1%	380	1.52	2.05	n.d. [f]	1700	1118
PS + *p*-T 1.5 + DCM (2) 0.01	564	3.08 (85.5) + 22.1 (14.5)	5.15	1300	1120	192
PS + *p*-T 1.5 + DCM (2) 0.03	574	3.27 (89.7) + 22.4 (10.3)	5.27	1500	1430	273
PS + *p*-T 1.5 + DCM (2) 0.05	578	3.42 (92.5) + 23.0 (7.5)	5.27	1300	1220	250
PS + 4-Br-*p*-T 1.5 + DCM (2) 0.03 + B 2	560	3.30	2.08	n.d.	360	109
PS + *p*-T 1.5 + 3 0.01	582	23.78	25.35	2330	2850	120
PS + *p*-T 1.5 + 3 0.03	590	27.35	40.71	2500	2560	94
PS + *p*-T 1.5 + 3 0.05	590	29.19	37.64	2460	2450	84
PS + *p*-T 1.5 + 4 0.01	578	7.27 (95.3) + 41.8 (4.7)	8.34	3670	4370	491
PS + *p*-T 1.5 + 4 0.03	582	9.52 (73.15) + 34.9 (26.85)	11.85	4400	4860	297
PS + *p*-T 1.5 + 4 0.05	592	9.44 (52.65) + 35.0 (47.35)	12.07	3700	4290	199
PS + *p*-T 1.5 + 5 0.01	582	10.82	12.94	3210	2510	232
PS + *p*-T 1.5 + 5 0.03	592	11.44	15.25	3240	3070	268
PS + *p*-T 1.5 + 5 0.05	596	11.59	13.50	3240	3220	278
PS + *p*-T 1.5 + 7 0.01	596	12.4	19.20	4250	3800	306
PS + *p*-T 1.5 + 7 0.03	602	13.8	20.74	4500	4610	334
PS + *p*-T 1.5 + 7 0.05	604	13.9	22.99	5070	5160	371
PS + *p*-T 1.5 + DANS 0.01	554	4.23	7.13	6280	6100	1442
PS + *p*-T 1.5 + DANS 0.03	570	4.40	7.68	5470	5390	1225
PS + *p*-T 1.5 + DANS 0.05	572	4.68	7.90	5480	5600	1196

[a] PS: polystyrene; *p*-T: *p*-terphenyl; 4-Br-*p*-T: 4-bromo-*p*-terphenyl; DCM: 4-(dicyanomethylene)-2-methyl-6-(4-dimethylaminostyryl)-4*H*-pyran; DANS: *trans*-4-dimethylamino-4′-nitrostilbene; B: benzophenone; P: piperidine; H: Hünig's base. The values of the first row are for the weight concentrations. The numbers in bold font refer to the red-emitting fluorophores described in Table 6. [b] values in radioluminescence. [c] estimated by beta-induced pulse height spectroscopy. The relative is calculated by a rule of thumb between BC-430 light yield reference [34]. [d] estimated by radioluminescence. The relative light yield is calculated by a rule of thumb between BC-430 light yield reference, its radioluminescence integral, and the other sample's integral. [e] the light yield recorded from radioluminescence was used in this calculation. [f] n.d.: not determined.

Having in hand promising materials with the use of DANS, it is noteworthy that this molecule can be quenched by amines or benzophenone as shown before. Thus, the same PS + *p*-terphenyl + DANS (0.01 wt %) were prepared with three different amounts of benzophenone, piperidine, or Hünig's base. Unfortunately, the time stability was not in favor to the scintillators loaded with the two amines. After almost 18 months of preparation, the materials suffered from intense visual degradation (Figure 5). The DANS molecule probably reacted with the amines since the emission spectra are totally different from the pristine materials. This visual information was confirmed by fluorescence spectroscopy, where all scintillators had almost the same fluorescence spectrum immediately after production, and Figure 6 shows their photophysical degradation. The blue shift of the emission spectrum is confirmed for the scintillators containing the amines only, with emission maxima located close to 470 nm for the two highest quenched scintillators (P4.8 and H4.8), when the neat or even the benzophenone-quenched scintillators keep their emission maxima close to 560 nm.

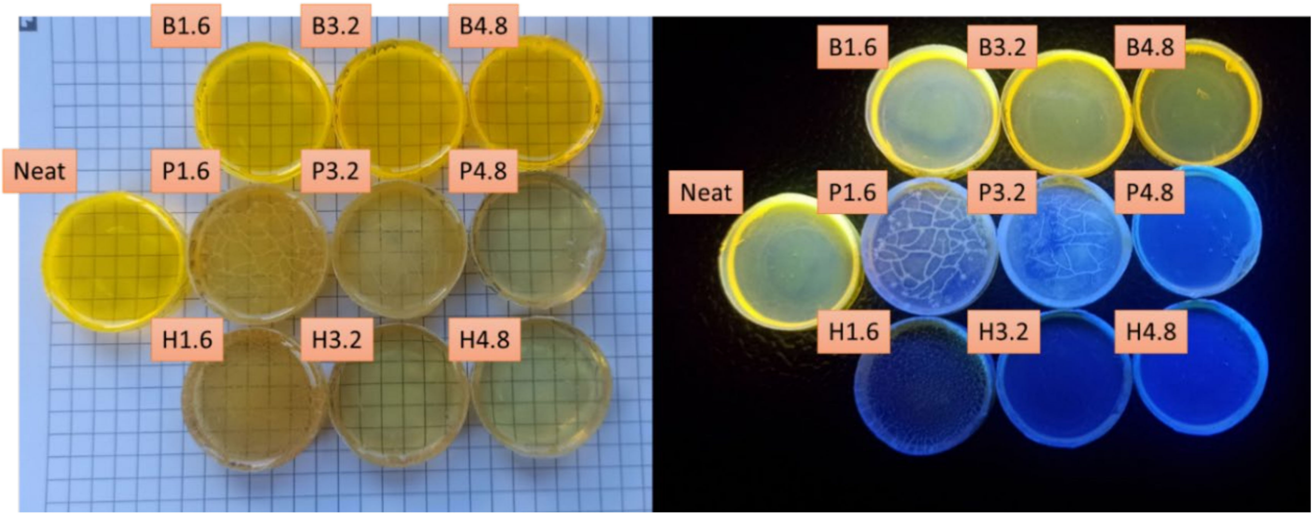

Figure 5. Scintillators composed of polystyrene containing *p*-terphenyl, DANS, and quenchers, under visible light (**left**) and 368 nm UV (**right**), pictured 18 months after preparation. B, P, and H stand for benzophenone, piperidine, and Hünig's base, respectively with their added concentration in wt %.

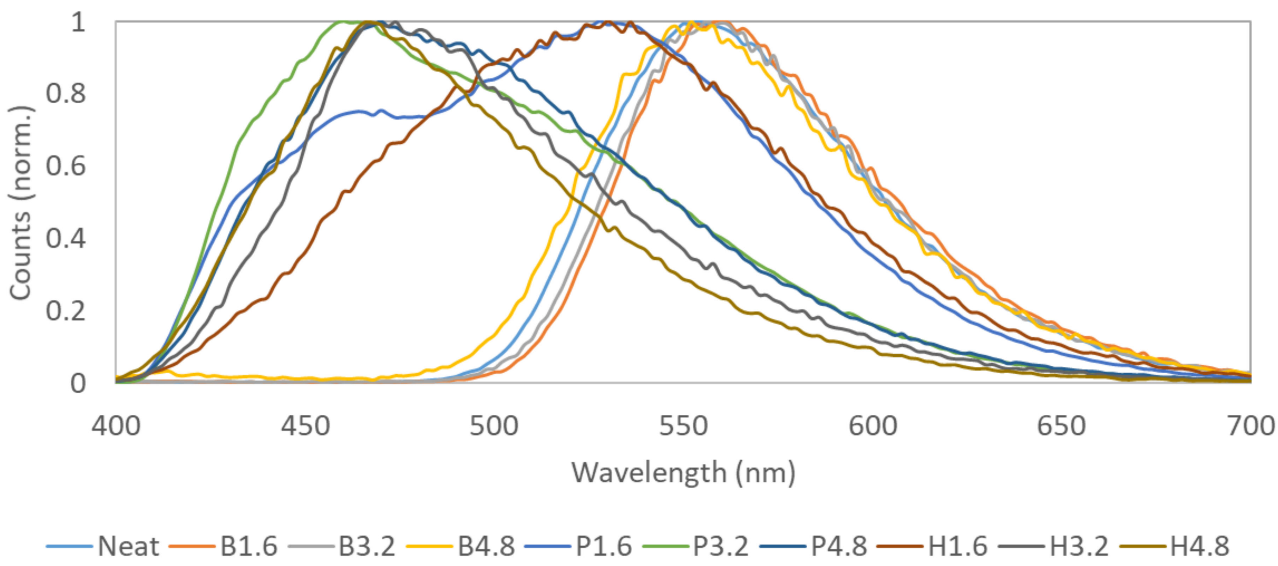

Figure 6. Fluorescence spectroscopy of *p*-terphenyl + DANS scintillators quenched with various amounts of quenchers: benzophenone (B series), piperidine (P series), or Hünig's base (H series). λ_{ex} = 370 nm. Values of the legend are in wt %.

4. Conclusions

Red and fast plastic scintillators have been decomposed into individual elements to better optimize their formulation. As a violet-emitting plastic scintillator, highly concentrated 4-bromo-*p*-terphenyl in polystyrene displays equal performances to BC-422Q 1%, but without the use of any quencher. This would allow a more stable material compared to previous studies about the time stability of quenched scintillators [22]. More than 4-bromo-*p*-terphenyl, several other molecules may act as nanosecond-range, UV-emitting fluorophore in a polymer matrix: oligophenylene family and several oxadiazoles among other.

It was awaited that adding a wavelength-shifter increases the decay time. However, two different orange-emitting molecules could fit our purpose: DCM and *trans*-4-dimethylamino-4′-nitrostilbene. DCM leads to very fast scintillators but with poor scintillating properties. *Trans*-4-dimethylamino-4′-nitrostilbene whose first use in the scintillation field (at least to the best of our knowledge) is described herein allocates both fastness and high light yield. For both fluorophores, mean decay time and FWHM in the range of 4 ns are obtained, which grant them the fastest scintillators with emission wavelength more than 550 nm ever described. Interestingly, *p*-terphenyl and DANS that are our final choice are both sensitive to quenching with amines. Comparing with commercial BC-430, a PS + *p*-T + DAANS configuration leads to a plastic scintillator with almost same light output but three times faster. Unfortunately, these scintillators were not stable with time when being quenched with piperidine or *N*,*N*-diisopropylethylamine. This work falls within recent efforts to find fast and red scintillators, whether organic or inorganic [35].

Funding: This project received funding from the Cross-Disciplinary Program on Instrumentation and Detection of CEA, the French Alternative Energies and Atomic Energy Commission. There was no external funding.

Institutional Review Board Statement: Not applicable.

Informed Consent Statement: Not applicable.

Data Availability Statement: Not applicable.

Acknowledgments: The author acknowledges the financial support of the Cross-Disciplinary Program on Instrumentation and Detection of CEA, the French Alternative Energies and Atomic Energy Commission.

Conflicts of Interest: The author declares that he has no known competing financial interests or personal relationships that could have appeared to influence the work reported in this paper.

References

1. Dujardin, C.; Hamel, M. Introduction—Overview on plastics and inorganic scintillators. In *Plastic Scintillators: Chemistry and Applications*; Hamel, M., Ed.; Springer Nature: Cham, Switzerland, 2021; pp. 3–33. [CrossRef]
2. Hamel, M.; Pjatkan, R.; Burešová, H. From the R&D to the commercialization of a new green-emitting plastic scintillator. *Nucl. Instrum. Methods A* **2020**, *955*, 163294. [CrossRef]
3. Franks, L.A.; Lutz, S.; Lyons, P.B. Development of Long-Wavelength-Emitting Scintillators with Improved Decay Time Characteristics. *IEEE Trans. Nucl. Sci.* **1978**, *NS-25*, 1024–1026. [CrossRef]
4. Beddar, S.; Tendler, I.; Therriault-Proulx, F.; Archambault, L.; Beaulieu, L. Recent Advances and Clinical Applications of Plastic Scintillators in the Field of Radiation Therapy. In *Plastic Scintillators: Chemistry and Applications*; Hamel, M., Ed.; Springer Nature: Cham, Switzerland, 2021; pp. 425–460. [CrossRef]
5. Gandini, M.; Villa, I.; Beretta, M.; Gotti, C.; Imran, M.; Carulli, F.; Fantuzzi, E.; Sassi, M.; Zaffalon, M.; Brofferio, C.; et al. Efficient, fast and reabsorption-free perovskite nanocrystal-based sensitized plastic scintillators. *Nat. Nanotechnol.* **2020**, *15*, 462–468. [CrossRef]
6. Ma, W.; Su, Y.; Zhang, Q.; Deng, C.; Pasquali, L.; Zhu, W.; Tian, Y.; Ran, P.; Chen, Z.; Yang, G.; et al. Thermally activated delayed fluorescence (TADF) organic molecules for efficient X-ray scintillation and imaging. *Nat. Mater.* **2021**, *21*, 210–216. [CrossRef] [PubMed]
7. Hamel, M.; Turk, G.; Rousseau, A.; Darbon, S.; Reverdin, C.; Normand, S. Preparation and characterization of highly lead-loaded red plastic scintillators under low energy X-rays. *Nucl. Instrum. Methods A* **2011**, *660*, 57–63. [CrossRef]
8. Cahill, P.A. Toward red-emitting, radiation tolerant chromophores. *Radiat. Phys. Chem.* **1993**, *41*, 351–363. [CrossRef]
9. Berlman, I.B.; Ogdan, Y.A. Fast red emitting plastic scintillator. *Nucl. Instrum. Methods* **1980**, *178*, 411–413. [CrossRef]
10. Montbarbon, E.; Amiot, M.-N.; Tromson, D.; Gaillard, S.; Frangville, C.; Woo, R.; Bertrand, G.H.V.; Pansu, R.B.; Renaud, J.-L.; Hamel, M. Large irradiation doses can improve the fast neutron/gamma discriminating capability of plastic scintillators. *Phys. Chem. Chem. Phys.* **2017**, *19*, 28105–28115. [CrossRef]
11. Hamel, M.; Trocmé, M.; Rousseau, A.; Darbon, S. Red-emitting liquid and plastic scintillators with nanosecond time response. *J. Lumin.* **2017**, *190*, 511–517. [CrossRef]
12. Tanaka, K.; Yanagida, T.; Hirose, A.; Yamane, H.; Yoshii, R.; Chujo, Y. Synthesis and color tuning of boron diiminate conjugated polymers with aggregation-induced scintillation properties. *RSC Adv.* **2015**, *5*, 966563. [CrossRef]
13. Ponomarenko, S.A.; Surin, N.M.; Borshchev, O.V.; Luponosov, Y.N.; Akimov, D.Y.; Alexandrov, I.S.; Burenkov, A.A.; Kovalenko, A.G.; Stekhanov, V.N.; Kleymyuk, E.A.; et al. Nanostructured organosilicon luminophores and their application in highly efficient plastic scintillators. *Sci. Rep.* **2014**, *4*, 6549. [CrossRef]
14. Huijun, Y.; Xiangtuo, W.; Yuying, J.; Yuanli, Z. Energy transfer in multi component plastic scintillators. *J. Lumin.* **1984**, *31-32*, 833–835. [CrossRef]
15. Dalla Palma, M.; Quaranta, A.; Marchi, T.; Collazuol, G.; Carturan, S.; Cinausero, M.; Degerlier, M.; Gramegna, F. Red Emitting Phenyl-Polysiloxane Based Scintillators for Neutron Detection. *IEEE Trans. Nucl. Sci.* **2014**, *61*, 2052–2058. [CrossRef]
16. Huijun, Y. Fast red-emitting plastic scintillators. *He Dianzixue Yu Tance Jishu. Yuanzineng Chubanshe: Beijing, China.* **1990**, *10*, 353–355.
17. Adadurov, A.F.; Zhmurin, P.N.; Lebedev, V.N.; Kovalenko, V.V. Plastic scintillator with phosphorescent dopants for α-particles registration. *Nucl. Instrum. Methods A* **2010**, *621*, 354–357. [CrossRef]
18. Sytnik, A.; Kasha, M. Spectroscopic criteria for wavelength shifting, fast, and red-infrared scintillators. *Radiat. Phys. Chem.* **1993**, *41*, 331–349. [CrossRef]
19. Tanaka, K.; Yanagida, T.; Yamane, H.; Hirose, A.; Yoshii, R.; Chujo, Y. Liquid scintillators with near infrared emission based on organoboron conjugated polymers. *Bioorg. Med. Chem. Lett.* **2015**, *25*, 5331–5334. [CrossRef] [PubMed]
20. Shakirova, J.R.; Grachova, E.V.; Melekhova, A.A.; Krupenya, D.V.; Gurzhiy, V.V.; Karttunen, A.J.; Koshevoy, I.O.; Melnikov, A.S.; Tunik, S.P. Luminescent Au^{I}—Cu^{I} Triphosphane Clusters That Contain Extended Linear Arylacetylenes. *Eur. J. Inorg. Chem.* **2012**, 4048–4056. [CrossRef]
21. Montbarbon, E.; Sguerra, F.; Bertrand, G.H.V.; Magnier, É.; Coulon, R.; Pansu, R.B.; Hamel, M. *N*-(2-ethylhexyl)carbazole: A new fluorophore highly suitable for liquid scintillation and n/γ discrimination. *Chem.-Eur. J.* **2016**, *22*, 12074–12080. [CrossRef]
22. Ebran, A.; Taieb, J.; Belier, G.; Chatillon, A.; Laurent, B.; Martin, J.-F.; Pellereau, E. Picosecond resolution on relativistic heavy ions' time-of-flight measurement. *Nucl. Instrum. Methods A* **2013**, *728*, 40–46. [CrossRef]
23. Moszyński, M. Study of light collection process from cylindrical scintillators. *Nucl. Instrum. Methods* **1976**, *134*, 77–85. [CrossRef]
24. Moszyński, M.; Bengtson, B. Status of timing with plastic scintillation detectors. *Nucl. Instrum. Methods* **1979**, *158*, 1–31. [CrossRef]
25. Nanoled, pulsed laser and LED light sources. Available online: https://www.horiba.com/us/en/scientific/products/fluorescence-spectroscopy/lifetime/tcspc-components/nanoled/nanoled-618/ (accessed on 17 January 2022).
26. Berlman, I.B.; Lutz, S.S.; Flournoy, J.M.; Ashford, C.B.; Franks, L.A.; Lyons, P.B. New fast organic scintillators using intramolecular bromine quenching. *Nucl. Instrum. Methods* **1984**, *225*, 78–84. [CrossRef]

27. Andreeshchev, E.A.; Avedisyan, V.S.; Veronyan, S.M.; Zyablin, V.L.; Kovyrzina, K.A.; Kushakevich, Y.P.; Rozman, I.M.; Shoniya, V.M. SPS-B18 high-speed plastic scintillator. *Instrum. Exp. Techn.* **1988**, *31*, 593–595, Translated from *Prib. Tekh. Eksp.* **1988**, 67–68.
28. Lutz, S.S.; Franks, L.A.; Flournoy, J.M. High speed liquid scintillators for optical fiber applications. *Nucl. Instrum. Methods* **1982**, *193*, 623–629. [CrossRef]
29. Zheng, H.; Baumbaugh, B.; Gerig, A.; Hurlbut, C.; Kauffman, J.; Marchant, J.; Pla-Dalmau, A.; Reynolds, K.; Ruchti, R.; Warchol, J.; et al. New scintillator and waveshifter materials. *AIP Conf. Proc.* **1998**, *450*, 371–380. [CrossRef]
30. Bondarev, S.L.; Knyukshto, V.N.; Stepuro, V.I.; Stupak, A.P.; Turban, A.A. Fluorescence and electronic structure of the laser dye dcm in solutions and in polymethylmethacrylate. *J. Appl. Spectrosc.* **2004**, *71*, 194–201, Translated from *Zh. Prikl. Spektrosk.* **2004**, *71*, 179–186. [CrossRef]
31. Muniz-Miranda, F.; Pedone, A.; Muniz-Miranda, M. Spectroscopic and DFT investigation on the photo-chemical properties of a push-pull chromophore: 4-Dimethylamino-4′-nitrostilbene. *Spectrochim. Acta Part A* **2018**, *190*, 33–39. [CrossRef] [PubMed]
32. Papper, V.; Pines, D.; Likhtenshtein, G.; Pines, E. Photophysical characterization of trans-4,4′-disubstituted stilbenes. *J. Photochem. Photobiol. A* **1997**, *111*, 87–96. [CrossRef]
33. Taniguchi, M.; Lindsey, J.S. Database of Absorption and Fluorescence Spectra of >300 Common Compounds for use in PhotochemCAD. *Photochem. Photobiol.* **2018**, *94*, 290–327. [CrossRef]
34. BC-430 plastic scintillator. Available online: https://www.crystals.saint-gobain.com/sites/imdf.crystals.com/files/documents/bc430-data-sheet.pdf (accessed on 17 January 2022).
35. Li, Y.; Chen, L.; Gao, R.; Liu, B.; Zheng, W.; Zhu, Y.; Ruan, J.; Ouyang, X.; Xu, Q. Nanosecond and highly Sensitive Scintillator Based on All-Inorganic Perovskite Single Crystals. *ACS Appl. Mater. Interfaces* **2021**, *14*, 1489–1495. [CrossRef] [PubMed]